Astron. Astrophys. 328, 321–330 (1997)

ASTRONOMY
AND
ASTROPHYSICS

β Pictoris light variations

II. Scattering by a dust cloud

H.J.G.L.M. Lamers[1,2], **A. Lecavelier des Etangs**[3,4], **and A. Vidal-Madjar**[3]

[1] Astronomical Institute, University of Utrecht, Princetonplein 5, 3584 CC, Utrecht, The Netherlands
[2] SRON Laboratory for Space Research, Sorbonnelaan 2, 3584 CA, Utrecht, The Netherlands
[3] Institut d'Astrophysique de Paris, CNRS, 98 bis boulevard Arago, F-75014 Paris, France
[4] NCRA, Tata Institute of Fundamental Research, Post Bag 3, Ganeshkhind, Pune University Campus, Pune 411 007, India

Received 9 December 1996 / Accepted 30 April 1997

Abstract. We explain the observed photometric variations of the star β Pic of November 1981 (Lecavelier et al. 1995) in terms of scattering and occultation by a dust cloud that is orbiting the star. The calculations were made for different phase functions for scattering and diffraction. We derived the parameters of the cloud that are compatible with the observed light curve: in particular the distance from the star (between 0.45 and 4 AU) and the effective scattering surface (a few times 10^{24} cm^2). However a spherical dust cloud is inconsistent with the observed photometric variations because its large size cannot explain the short duration of the dip in the light curve. A model consisting of a flat cloud, that is elongated in the orbital plane and has a pointed shape with the largest optical depth closest to the star, can explain the light curve. We suggest that such a cloud could be the result of one large comet that passes the line of sight to the star near periastron, or of a fragmented comet of the type as the Shoemeker-Levi fragments. The model suggests that the comet passes the star at a distance of about 0.4 AU and a dust mass of about 2×10^{21} g. The crucial test of these models is the possible presence (in the case of an orbiting dust cloud) or absence (in the case of a comet) of periodic recurrences of the short time photometric variations.

Key words: stars: β Pic – circumstellar matter – dust – scattering – comets: general

1. Introduction

The star β Pic is surrounded by a dust-ring that was first discovered by the IRAS satellite due to its large IR-flux (Aumann et al. 1984). High resolution optical observations by Smith and Terrile (1984), Paresce and Burrows (1987) and Golimowski et al. (1993) and infrared images by Lagage and Pantin (1994) shows that the disk is seen almost edge-on and that it has a central clearing zone, which extends to about 20 AU from the star and contains little dust. The star is one of the best candidates for the detection of an extra-solar planetary system. (For an excellent recent review, see Artymowicz 1995).

Recently Lecavelier et al. (1995) have reported the discovery of fast photometric variations of β Pic observed with the Geneva photometric system between Nov 1 and Nov 16 1981. During this period the star brightened in five days by about 0.06 magnitude, dropped back to approximately its normal brightness within a few hours, increased again by 0.02 magnitude within one day, and than slowly decreased to its normal magnitude in about 5 days. The star has been monitored photometrically with the Danish telescope at ESO from JD 2450030 to JD 2450070 and from JD 2450090 to JD 2450130, i.e. during an interval of 100 days, with a 20 day gap (Lecavelier 1996). No photometric variations larger than about 0.005 mag occurred during this interval. So *if* the variability is recurrent, its recurrence time is larger than 100 days (We ignore the very small possibility that the short term variations occurred exactly during the 20 day gap in the observations.)

Lecavelier et al. (1995) and (1996, Paper I) suggested that this variation could be explained in terms of a hole in a ring around β Pic due to a putative planet, and occultation of the star by this planet. When the hole is in front of the star the circumstellar extinction decreases and the star is brighter. The dip is due to occultation of the star by the planet. The problem with this interpretation is that it requires a substantial extinction of the star of at least about 0.06 mag by a rather narrow dust ring at the distance of the planet and with a width of about twice its Hill-radius, i.e. about 0.5 AU for a planet of a Jupiter mass at a distance of 5 AU. There is no evidence for the existence of such a narrow ring with a substantial extinction. Moreover, the explanation of the dip in the lightcurve by occultation of a planet at a distance of about 5 AU requires a very small tilt angle of the orbital plane of less than 0.1 degree.

Therefore we investigate in this paper the alternative possibility of scattering and occultation due to a dust cloud that is orbiting the star. The increase in brightness is due to forward

Table 1. The stellar parameters

Distance	19.2 ±0.2	pc
Luminosity	8.7 ±0.6	$L_\odot$
Effective T	8200 ± 150	K
Radius	1.46 ± 0.14	$R_\odot$
Mass	1.8 ±0.1	$M_\odot$
v sin$i$	100	km s^{-1}

scattering when the cloud is almost in front of the star and the dip is due to occultation of the star by part of the cloud. In Sects. 2 and 3 we discuss the stellar parameters and the light curve of β Pic. In Sect. 4 we derive the parameters for a spherical dust cloud that produces the observed lightcurve. In Sect. 5 we describe the effect of scattering by an idealized comet and we derive the parameters of this comet. Sect. 6 gives a critical discussion of the results and the strong and weak points of this interpretation of the photometric variations of β Pic.

2. The stellar parameters

We adopt the stellar parameters of β Pic from Lanz et al. (1995) and the revisions for the new distance of 19.3±0.2 pc, measured with *Hipparcos* (Crifo et al. 1997). They are listed in Table 1. With the mass of 1.8 $M_\odot$ the Keplerian velocity of a circular orbit at a distance d from the star is

$$v_{\rm circ} = 40\ d(AU)^{-1/2} \quad \text{km s}^{-1} \tag{1}$$

and the period is

$$P = 272\ d(AU)^{3/2} \quad \text{days.} \tag{2}$$

3. The lightcurve around JD 2444920

The lightcurve in the Geneva system (from Lecavelier et al. 1995) in V, $U-B$ and $B-V$ is shown in Fig. 1. Following Lecavelier et al. we only use the most reliable photometry (with $w \geq 3$). The V magnitude has an uncertainty of 1 $\sigma \simeq 0.005^m$. The colours have an uncertainty of 1 $\sigma \simeq 0.0035^m$. Notice that the colours hardly show any variation within 0.002^m during the visual brightening and fading of the star with the exception of the spike in $U-B$ at JD 4918.628 (and also at JD 4918.563, but with a bad quality : $w = 0$). [1] This shows that our error estimate is rather conservative (Lecavelier et al. 1995). The spike in $U-B$ deviates from the mean by only 3 σ. However, if we take the colour variations over the period of 15 days as a more realistic estimate of their errors we find values of $\sigma(U-B) = 0.0013^m$. In that case the spike in $U-B$ deviates by 10 σ from the mean constant value. We conclude that the colours are constant during the photometric variability within the observational uncertainty, except the $U-B$ peak at JD 4918.628.

This constant colour is also found for the other Geneva colours that are not shown here. The achromatic behaviour of the optical light variations suggests that it is caused by scattering or absorption by dust grains with a size considerably larger than the wavelength of the light. The change in the $U-B$ colour at JD 4918.628 shows that the light curve at this epoch is caused by some other effect than the achromatic scattering that may produce the rest of the light curve. We will show later that diffraction of light may explain the change in the $U-B$ colour.

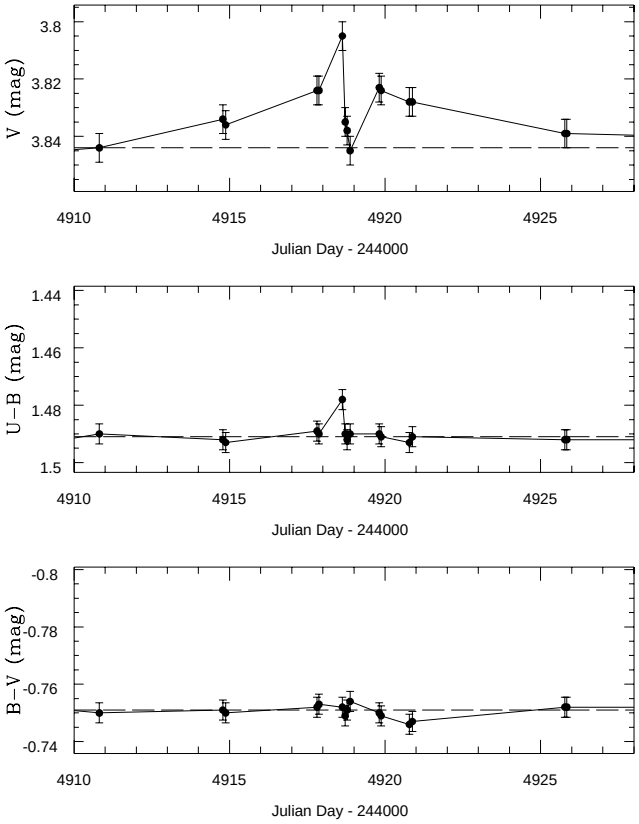

Fig. 1. The light curve of β Pic observed in Geneva photometry around JD 4920, November 1981 (from Lecavelier et al. 1995). The top figure shows the variations in V and the lower figures show the variations in $U-B$ and in $B-V$. The conservative estimates of the uncertainty is $\sigma \simeq 0.005^m$ in V and 0.0035^m in the colours, but the real uncertainty in the colours may be a factor 2 smaller. Notice that the colours are constant, except the one peak in $U-B$ at JD 4918.628.

At first glance the V-lightcurve looks asymmetric. However, this might be due to the specific times of the observations. Test calculations show that the data can very well be fitted to a symmetrical lightcurve of which the predicted second high peak of $V \simeq 3.80$ was missed.

It is interesting that the star reached about its normal magnitude during the central minimum. However, we cannot exclude the possibility that it briefly dropped to lower than normal magnitude shortly after JD 4918.86, which is the epoch of the deepest point in the light curve.

The duration of the dip in the lightcurve is at most 1.17 days, i.e. the separation between the two high points at JD 4918.628 and 4919.802, and at least 0.46 days, i.e. twice the time between the highest point at JD 4918.628 and the deepest point at JD 4918.856. In the rest of the paper we adopt a duration of the dip of 0.8 ± 0.4 days, and a FWHM of the dip of 0.4 ± 0.2 days.

[1] We indicate the Julian Dates by JD - 244000

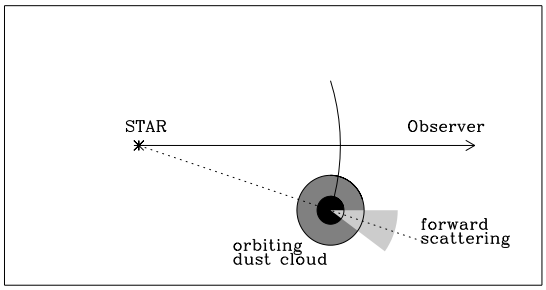

Fig. 2. A picture of a spherical dustcloud orbiting the star at a distance d. The cloud is optically thin but it has an optically thick core. The forward scattering angle of the phase function is shown schematically.

4. Some simple estimates for a spherical scattering cloud

We first consider the effect of a spherically symmetric scattering cloud, that is orbiting the star, on the lightcurve. In this section we start with some very simple estimates in order to derive the ranges of parameters that are compatible with the observed light curve.

Suppose that the dust cloud has a projected effective scattering area $\Sigma_{\rm sca}$, and orbits the star at a distance d. The central part of the projected area may be optically thick, with an effective scattering surface $\Sigma_{\rm sca}^{\rm thick}$, and the outer parts may be optically thin with a surface $\Sigma_{\rm sca}^{\rm thin}$, with $\Sigma_{\rm sca} = \Sigma_{\rm sca}^{\rm thick} + \Sigma_{\rm sca}^{\rm thin}$. Here "optically thick" and "thin" mean that the optical depth for a line of sight through the cloud is $\tau > 1$ or < 1 respectively. The definitions are explained in terms of the particle distribution for a spherical cloud in Appendix (A). Similarly, the cloud has a projected effective extinction surface area $\Sigma_{\rm ext}$. The schematic model is shown in Fig. 2.

We assume that the distance d of the cloud is much larger than the radius of the star and the radius of the cloud. This is justified because we expect $d \simeq$ a few AU and the radius of the cloud to be on the order of a stellar radius or smaller. In that case the radiation from the star to the cloud can be considered as a parallel beam and the radiative transfer is simple.

4.1. The brightness variations due to an orbiting cloud

The flux of scattered light (i.e. starlight scattered by the dustcloud) that reaches the earth is

$$f_\nu^{\rm sca}(\Theta) \equiv \frac{L_\nu^*}{4\pi d^2} \cdot \left\{ \Sigma_{\rm sca}^{\rm thin} P(\Theta) \; + \Sigma_{\rm sca}^{\rm thick} \frac{1}{4\pi} \right\} \frac{1}{a^2} \qquad (3)$$

where L_ν^* is the stellar monochromatic luminosity, and a is the distance of the star from the earth. The phase function of the scattering is $P(\Theta)$, where Θ is the angle at the position of the cloud between the direction to the star and to the earth. The phase function is normalized to $\int P(\Theta) d\Omega = 1$. The first factor is the flux of stellar radiation at the distance of the cloud. The second factor is the amount of radiation that is scattered by the cloud in the direction of the observer per steradian. The last factor converts this into a flux at the earth. We assume that the optically thick part of the dustcloud scatters isotropically, $P(\theta) = (4\pi)^{-1}$, and the optically thin part scatters with the phase function. This means that the variation of the brightness reflects the variation of the scattering phase function as the cloud passes the line of sight from the star to the observer.

The flux from the star that reaches the observer directly is $f_\nu^* = L_\nu^*/4\pi a^2$ so the normalized scattered flux is

$$\frac{f_\nu^{\rm sca}(\Theta)}{f_\nu^*} = \frac{\Sigma_{\rm sca}^{\rm thin} \cdot P(\Theta) + \Sigma_{\rm sca}^{\rm thick}/(4\pi)}{d^2} \qquad (4)$$

Here we have assumed that if the brightness of the star is reduced by extinction in the disk around β Pic, the scattered radiation from the cloud is reduced by the same extinction, so the ratio is independent of the extinction. Equation (4) describes the variation of the scattered flux as a function of Θ, i.e. as a function of the orbital phase of the cloud outside occultation. For $\Theta \simeq \pi$ the cloud is approximately behind the star and for $\Theta \simeq 0$ the cloud is approximately in front of the star as seen by the observer.

The dust disk around β Pic is almost seen edge-on with a tilt angle $t \leq 3$ degrees (Artymowicz, 1995; Kalas and Jewitt, 1995). This implies that the orbiting cloud which moves in the plane of the dust disk might partly obscure the star at $\Theta \simeq 0$. The fraction of the stellar flux that is removed by extinction when the dust cloud is in front of the star is

$$\frac{f_\nu^{\rm occ}(\Theta)}{f_\nu^*} = \frac{\Sigma_{\rm occ}(\Theta)}{\pi R_*^2} \qquad (5)$$

where $\Sigma_{\rm occ}(\Theta)$ is the projected effective scattering area of the part of the cloud that occults the star. This area depends on the azimuthal position of the cloud in its orbit and hence on the scattering angle Θ (see Appendix).

The brightness variation of β Pic due to the orbiting dust cloud is described by

$$\frac{f_\nu(\Theta)}{f_\nu^*} = 1 + \frac{f_\nu^{\rm sca}(\Theta)}{f_\nu^*} - \frac{f_\nu^{\rm occ}(\Theta)}{f_\nu^*} \qquad (6)$$

For $\Theta \simeq \pi$ the flux will increase due to back scattering of the stellar radiation by the dust cloud. This scattered flux will (partly) disappear when the cloud is occulted by the star. For $\Theta \simeq 0$ the flux will increase due to forward scattering of the stellar radiation by the cloud and the flux from the star will be reduced when the cloud occults part of the star. The amount of brightening near $\Theta \simeq 0$ or $\Theta \simeq \pi$ depends strongly on the phase function for forward or backward scattering by the cloud. We will show below that the observed brightening cannot be explained by backward scattering because $P(\pi)$ is too small for reasonable values of the phase function. Therefore we concentrate on the explanation of the observed brightness variation of β Pic in terms of forward scattering and occultation when the cloud is almost in front of the star.

4.2. The phase function for scattering

We adopt a Henyey-Greenstein (HG) phase functions for scattering.

$$P(\Theta) = \frac{1}{4\pi} \frac{1 - g^2}{\{1 + g^2 - 2g\cos\Theta\}^{3/2}} \qquad (7)$$

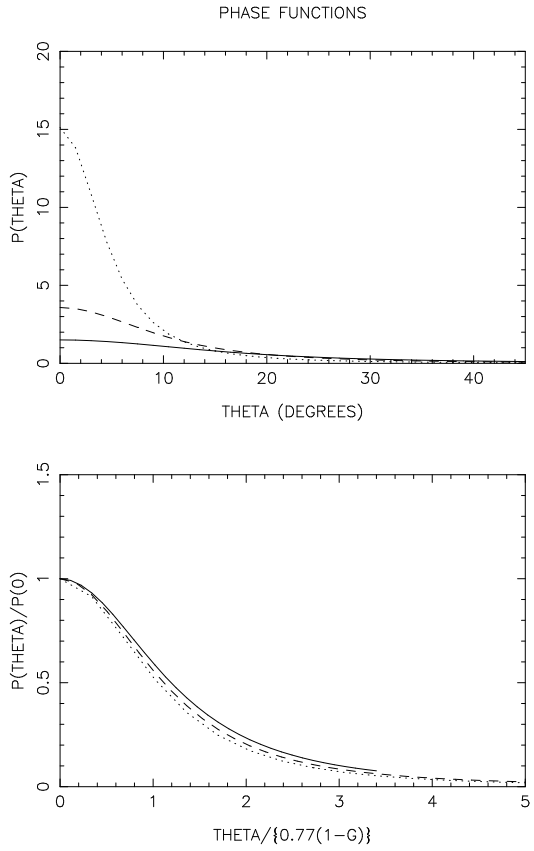

Fig. 3. The Henyey-Greenstein phase functions for forward scattering with g = 0.7 (full line), 0.8 (dashed line), and 0.9 (dotted line). The upper figure shows the phase functions. The middle figure shows the same phase functions, normalized in $P(\Theta)$ to the maximum value and in Θ to the approximate halfwidth of $0.77(1-g)$. Notice that the normalized curves are very similar.

which is normalised to $\int P(\Theta)d\Omega = 1$. The factor g is equal to the mean scattering angle $< \cos\Theta >$, with $g > 0$ for forward-peaked scattering functions and $g < 0$ for backward-peaked scattering functions. We assume that the particles of the dust cloud mainly scatter in the forward direction, so $g > 0$.

Fig. 3A shows the phase functions for $g = 0.7, 0.8$ and 0.9 and Fig. 3B shows the same phase functions, but normalized in amplitude to their maximum value of

$$P(0) = \frac{1}{4\pi}\frac{1+g}{(1-g)^2} \tag{8}$$

and in Θ to their halfwidth $\Theta_{1/2}$ where $P(\Theta_{1/2}) = P(0)/2$. For strongly forward peaked scattering, $g \geq 0.7$, the half maximum is reached at

$$\Theta_{1/2} \simeq 0.77(1-g) \tag{9}$$

We will use this property for our simple estimate of the parameters of the orbiting cloud that may explain the observed lightcurve. Notice that the shape of the phase functions is similar to the gradual rise and fall of the light curve in Fig. 1.

In order to have an impression of the value of g for realistic phase functions, we consider two specific cases: the phase function of scattering by the Zodiacal dust in the solar system and the phase function for diffraction by micron-size particles.

4.2.1. The phase function for the Zodiacal dust

The study of the Zodiacal light in the solar system shows that the dust has a phase function that can be described as a linear combination of three Henyey-Greenstein functions

$$P_{\rm zod}(\Theta) = \sum_{k=1}^{3} w_k \Phi_{\rm HG}(\Theta, g_k) \tag{10}$$

where $\Phi_{\rm HG}$ are the Henyey-Greenstein functions with $g_1 = 0.70$, $g_2 = -0.20$ and $g_3 = -0.81$ and the weight factors are $w_1 = 0.665, w_2 = 0.330$ and $w_3 = 0.005$ (Hong, 1985). This phasefunction has a value of $P(0) = 1.005$ for forward scattering. The phase function is shown in Fig. 5a. For small scattering angles of less than about 10 degrees, this phase function can be approximated by a single HG-function with $g \simeq 0.64$. The efficiency factor for scattering in the visual is about $Q_{\rm sca} \simeq 2$.

4.2.2. The phase function of diffracting particles

We calculated the diffracting part of the phase function with a mixture of particles with a size distribution of $n(r) \sim r^{-3.5}$ with a minimum radius r_1 and a maximum radius of r_2, where $n(r)$ is the number of particles as a function of their radius r. Following Pollack & Cuzzi (1980), the phase function for diffraction at wavelength λ is given by

$$P(\theta) = \int_{r_2}^{r_1} D(\tilde{x},\theta)\pi\tilde{x}^2 n(\tilde{x})d\tilde{x} \tag{11}$$

with

$$D(\tilde{x},\theta) = C_D \frac{\tilde{x}}{4\pi}\left(\frac{2J_1(\tilde{x}\sin\theta)}{\tilde{x}\sin\theta}\right)^2 \frac{1+\cos^2\theta}{2} \tag{12}$$

where $\tilde{x} = 2\pi r/\lambda$ and C_D is obtained from the normalization $\int P(\theta)d\Omega = 1$.

Fig. 4 shows the phase functions for two distributions with $r_1 = 0.3\mu m$, $r_2 = 5\mu m$ (mixture A) and for slightly larger particles with $r_1 = 2\mu m$, $r_2 = 10\mu m$ (mixture B). Notice that these functions are very strongly peaked forward and reach values of $P(0) > 15$ for mixture A and $P(0) > 100$ for mixture B. For small phase angles the phase functions can be approximated by a HG-function with $g = 0.90$ (in V) and $g = 0.94$ (in U) for mixture A and $g = 0.96$ (in V) and $g = 0.99$ (in U) for mixture B. The phase functions at small angles are about twice as high in the UV than in the visual. We will use this property later to explain the peak in the $U-B$ lightcurve of Fig. 1. The efficiency factor for diffraction is $Q_{\rm diff} = 1$.

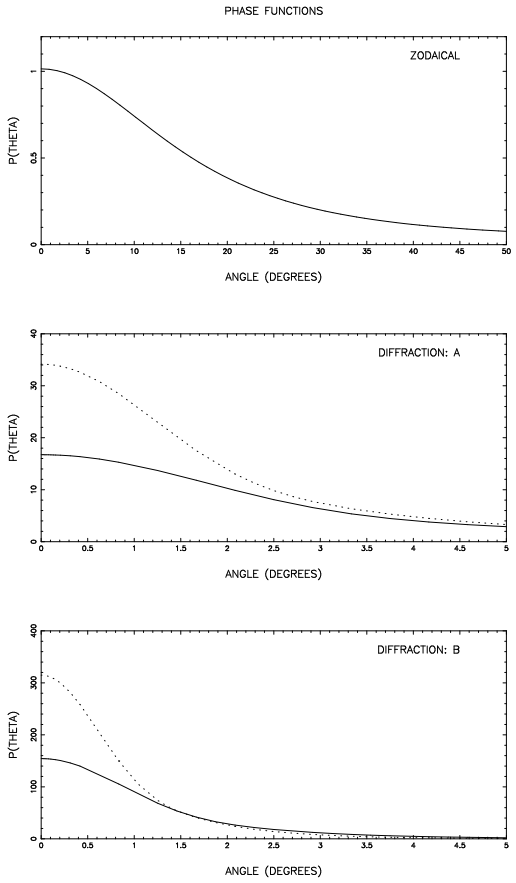

Fig. 4. The phase functions for the scattering by Zodiacal dust and for the diffraction by mixtures A and B. The phase function for diffraction is given for two wavelengths: 5000 Å (full line) and 3500 Å (dotted line). All phase functions are normalized to $\int P(\Theta)d\Omega = 1$. Notice the very strong peaking of the phase functions for diffraction

4.2.3. The adopted phase functions

Based on the arguments given above we will approximate the phase function throughout this paper by a HG-function, with g as a free parameter. We expect g to be in the range of 0.6, for scattering with an efficiency factor $Q \simeq 2$, to about 0.9 to 0.98 for diffraction with an efficiency factor $Q \simeq 1$.

4.3. Comparison of the simple model predictions with the observed lightcurve

In this section we derive some rough estimates for the dust cloud from the comparison between the expected and the observed photometric variations.

4.3.1. The width of the brightness increase in the lightcurve

Fig. 1 shows that the maximum brightness increase at the center of the lightcurve at JD 4918.8 would have been about -0.05 $\pm$ 0.01^m if there was no central absorption. In our model this brightness increase is due to the scattering by the optically thin part of the dust cloud at phase function $P(\Theta = 0)$. The lightcurve also shows that the half maximum of the phasefunction is reached about 3.0$\pm$0.5 days before and after the central dip. This corresponds to an orbital phase of $\Theta_{1/2}$ (Eq 9) so the orbital period P and the scattering parameter g are related via

$$\frac{\Theta_{1/2}}{2\pi} P = 3^d.0 \pm 0^d.5 \tag{13}$$

or

$$P \simeq \frac{2\pi}{0.77} \frac{3.0}{(1-g)} \simeq \frac{24 \pm 4}{1-g} \text{ days} \tag{14}$$

The orbital period depends on the mass of the star and the distance of the cloud d (Eq. 2). Combination of Eqs. (14) and (2) gives a relation between the distance of the cloud and g

$$d(AU) \simeq (0.20 \pm 0.02)(1-g)^{-2/3} \tag{15}$$

that explains the FWHM of the brightness increase of β Pic. For g = 0.70, 0.80, 0.90, 0.95 and 0.98 we find distances of 0.45, 0.58, 0.93 , 1.5 and 2.7 AU respectively. Notice that the distance increases with increasing g, i.e. for more strongly forward peaked phase functions. These values are actually upper limits, because we have assumed that the linear dimension of the cloud is much smaller than the distance d so that the radiation from the star can be approximated by a parallel beam. The distances have to be slightly smaller if the angular size of the dust cloud is properly taken into account. This is due to the fact that the finite angular size of the cloud as seen from the star results in a light curve that is due to the convolution of the phase function with the angular size. The resulting net broadening of the phase function requires that the cloud must have a slightly higher angular velocity around the star (i.e. a smaller distance to the star) to produce the observed width of the brightness increase.

The distance of the orbiting dust cloud that is consistent with the width of the lightcurve is less than about 1 AU, unless the dust in the cloud has an extremely forward peaking phase function due to diffraction. Only in that case can the distance be a few AU.

4.3.2. The maximum brightness increase

The maximum of the lightcurve, without the central dip, is about $0^m.05$ brighter than the star. The maximum predicted brightness at Θ = 0, without the occultation, is given by Eqs. (4) and (6)

$$-\Delta m^{\rm max}_{\rm pred} = 2.5 \log \left\{ 1 + \frac{f^{\rm sca}_\nu(0)}{f^*_\nu} \right\} \simeq \frac{f^{\rm sca}_\nu(0)}{f^*_\nu} = \frac{\Sigma^{\rm thin}_{\rm sca} \cdot P(0) + \Sigma^{\rm thick}_{\rm sca}/(4\pi)}{d^2} \tag{16}$$

Using the expression (8) for the phase function $P(0)$ and Eq. (15) for the relation between d and g, and making the reasonable assumption that the larger part of the cloud is optically thin (otherwise the forward scattering would be inefficient) so $\Sigma^{\rm thick}/(4\pi) < \Sigma^{\rm thin} P(0)$, we find an estimate for the projected scattering surface of the cloud

$$\Sigma^{\rm thin}_{\rm sca} \simeq 1.2\, 10^{25} \frac{(1-g)^{2/3}}{(1+g)} \text{ cm}^2 \tag{17}$$

Table 2. The parameters of the spherical cloud

Phase function	Dist	Period	$\Sigma_{\rm sca}^{\rm thin}$	$r_{\rm sca}^{\rm thin}$ τ = 0.5	$r_{\rm sca}^{\rm thin}$ τ = 0.01
g	AU	days	cm^2	R_*	R_*
0.60	0.37	61	3.8 10^{24}	15.0	95
0.70	0.45	82	2.9 10^{24}	13.2	83
0.80	0.58	120	2.2 10^{24}	11.3	71
0.90	0.93	244	1.3 10^{24}	8.8	55
0.95	1.47	485	7.8 10^{23}	6.8	43
0.98	2.71	1210	4.2 10^{23}	5.0	32

This results in a projected scattering surface of the optically thin part of the cloud of $\Sigma_{\rm sca}^{\rm thin}$ between 3.8 10^{24} and 4 10^{23} for $0.60 < g < 0.98$ (see Table 2). This is a large projected surface since it is between 100 and 15 times the projected surface πR_*^2 of the star.

The linear radius $r_{\rm sca}$ of the cloud depends on the projected scattering surface as

$$\Sigma_{\rm sca}^{\rm thin} \simeq \pi r_{\rm sca}^2 < 1 - e^{-\tau} > \qquad (18)$$

where the second factor is averaged over the projected surface of the optically thin region of the cloud (see App. A). The radius of a spherical cloud is given in Table 2 for τ = 0.5 and τ = 0.01. If the cloud is flattened in the orbital plane the linear dimension of the cloud in the orbital plane must be larger than these values for the cloud to have a sufficiently large scattering surface.

4.4. The dip due to occultation of the star

The dip in the lightcurve could be the result of the occultation of part of the stellar disk by the cloud. For a spherical cloud of radius $r_{\rm cloud}$ that passes exactly in front of the star, the occultation will last $2(r_{\rm cloud}+R_*)/v_{\rm circ}$. Adopting the values of $r_{\rm cloud} \simeq r_{\rm sca}^{\rm thin}$ (Table 2) derived above from the observed brightening, we find that the occultation is expected to last about 6 days. This is about ten times longer than the FWHM of the observed dip in the lightcurve. The expected occultation time could be smaller if the orbit is slightly tilted so that the star is only occulted by the upper or lower rim of the cloud. This however requires that the path of the star is only one percent below the rim of the cloud. We think that this is an unlikely coincidence.

The alternative way to explain the short duration of the dip and the steep brightness decrease after the brightening is to assume that the cloud consists of two very distinct parts: a large region which is optically very thin and produces the brightening but no noticable extinction as it passes in front of the star, and a smaller core which is optically thicker that produces the dip. The optically thin region should be very optically thin, $\tau < 0.01$, to avoid the onset of the dip long before it is observed. This requires a geometrically very extended region (Table 2). The optically thick core should have a radius of $1.2 < r^{\rm thick} < 0.2 R_*$ for a distance range of $0.37 < d < 2.7$ AU to explain the duration of the dip. If the optically thick center of the cloud is larger than about 1 R_* its optical depth should be about 0.04 to explain the depth of the dip. On the other hand, if the radius is only 0.2 R_*, the optical depth should be larger than 1.

4.5. Conclusions of the simple spherical model

1. The scattering phase function of the dust must be strongly peaked forward in order to explain the brief duration of the photometric event and the increase in brightness.
2. The distance of the dust cloud together with the phase function indicates that the cloud must be within 0.37 to 1.0 AU if $g \simeq 0.60$ to 0.90, with larger distances corresponding to higher values of g. For very strongly peaked phase functions due to diffraction with $g \simeq 0.95$ to 0.98 the distance of the dust cloud is between 1.5 and 2.7 AU.
3. The projected surface of the optically thin part of the dust cloud is between 4 10^{24} and 4 10^{23} cm^2, depending on the distance. The optical depth must be very small $\tau < 0.01$ to avoid a very long dip. The radius of the cloud is between 95 and 32 R_*.
4. A large optically thin cloud of radius about 50 R_* at a distance of about 1 AU $\simeq$ 150 R_* will not be spherically symmetric, but it will most likely be flat (in the orbital plane) and elongated by radiation pressure. Therefore we consider below the lightcurve caused by forward scattering scattering in an elongated "cometary cloud".

5. A cometary cloud

To explain the observed lightcurve in the context of a scattering cloud requires a large optically thin cloud (to produce the observed brightening) with an optically thick area closest to the star (to produce the short occultation time). Such a model resembles the geometry of a comet, consisting of an optically thick nucleus and an optically thin dust tail. In this section we consider a model that schematically describes a comet that is passing close to the line of sight to the star. We assume that the comet has a parabolic orbit and that we see it passing the star near periastron. This means the the orbital velocity is a factor $\sqrt{2}$ larger than given by Eq. 1.

5.1. The schematic model

The model consists of a slab of dust of constant thickness h that has a sectorial (almost triangular) shape with the head of the triangle pointed to the star. The triangle has a half opening angle α and a length L. The vertical optical depth for scattering through the slab depends on the distance l from the "head" of the triangle and is $\tau_{\rm sca}(l)$. The slab moves in its orbital plane. As the comet passes the star, the head remains pointed to the star and the tail remains pointed away from the star. This last assumption is not essential to the model. The model is depicted in Fig. 5.

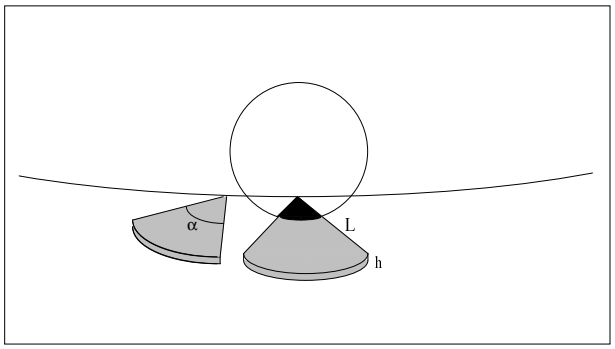

Fig. 5. The schematic model of a comet, in an orbital plane that passes closely to the line of sight to the star

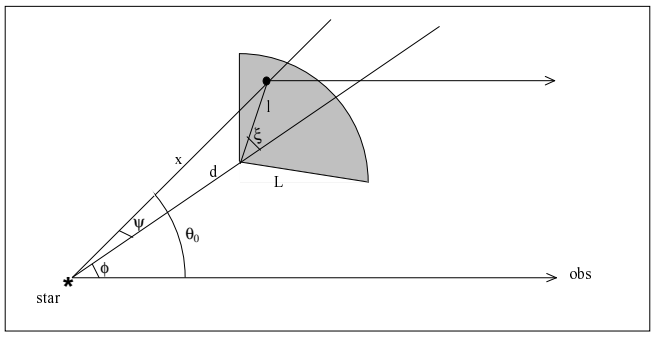

Fig. 6. The coordinate system of the triangular comet model

The density distribution in the cometary cloud is described by the vertical optical depth $\tau_{\rm sca}(l)$. We adopted the following parameterization

$$\tau_{\rm sca}(l) = \frac{l_0}{l} \quad \text{for} \quad l > \frac{l_0}{\tau_{\rm max}} \tag{19}$$

and

$$\tau_{\rm sca}(l) = \tau_{\rm max} \quad \text{for} \quad l < \frac{l_0}{\tau_{\rm max}} \tag{20}$$

where we have set $\tau_{\rm max} = 3$. This distribution has the property that the particle density in the slab decrease with distance from the head of the comet as l^{-1}, which is equivalent to assuming a constant dust production rate. The value of $\tau_{\rm max}$ avoids the column density to become infinite near the nucleus at $l = 0$.

The projected scattering surface of the region of the cloud where $\tau_{\rm sca} < 3$ is

$$\Sigma_{\rm sca} = \alpha l_0 (L - l_0/\tau_{\rm max}) \simeq \alpha l_0 L \tag{21}$$

The coordinate system of the triangular comet is shown in Fig. 6. The azimuthal angle of the comet with respect to the line of sight to the observer is ϕ. The location of any point in the comet is given by the angle ξ with respect to the bisector and the distance l from the head. The line from the star to that point makes an angle ψ with respect to the line from the head of the comet to the star with

$$\psi = \arctan\left\{\frac{l.\sin\,\xi}{d + l.\cos\,\xi}\right\} \tag{22}$$

The distance x from the center of the star to any point in the comet is

$$x = d\sqrt{1 + \frac{2l}{d}\cos\,\xi + \left(\frac{l}{d}\right)^2} \tag{23}$$

If the observer is in the plane of the orbit, the scattering angle from any point in the cloud to the observer is Θ_0 with

$$\Theta_0 = \phi + \psi \tag{24}$$

If the plane of the comet is tilted with respect to the observer by an angle t, the scattering angle is

$$\Theta = \arccos(\cos\,\Theta_0 \cdot \cos\,t) \tag{25}$$

5.2. Scattering and occultation by the comet cloud

The flux of the star, scattered to the earth by the comet is

$$\frac{f_{\rm sca}}{f^*} = \frac{1}{d^2}\int_0^\alpha \int_0^L \left(\frac{d}{x}\right)^2 \left\{1 - e^{\tau_{\rm sca}(l)/\sin t}\right\} P(\Theta) \sin\,t\; l.dl \cdot d\alpha \tag{26}$$

Here we have explicitly assumed that the comet is flat in the plane of its orbit with h/d smaller than the half width of the scattering phase function.

If the comet is in front of the star, the comet head will occult the star. Any surface element of the projected comet in front of the stellar disk will produce an extinction by a factor $e^{-\tau_{\rm ext}}$, where $\tau_{\rm ext} = \tau_{\rm sca}(l)(A/Q_{\rm sca})/\sin\,t$, where A is the albedo. The condition for a surface element of the comet to be in front of the star is

$$x^2(\sin^2\Theta_0 + \cos^2\Theta_0 \cdot \sin^2 t) < {R_*}^2 \tag{27}$$

5.3. The dust production rate and the mass of the dust tail

The mass of the comet tail $M_{\rm ct}$ is related to the distribution of the vertical optical depth through the tail. For spherical dust grains of radius r the total mass is

$$M = \int dM_{\rm ct}(l)dl = \int \frac{4}{3}\pi r^3 \rho \alpha l N(l) dl \tag{28}$$

where ρ is the density in the dust grains and $N(l)$ is the vertical number density of the particles through the tail, which is related to the optical depth $\tau_{\rm sca}(l)$ via

$$N(l) = \frac{\tau_{\rm sca}(l)}{4\pi r^2 Q_{\rm sca}} \tag{29}$$

Table 3. The parameters of the cometary cloud

Phase function	Dist	α	l_0	t	$P/\Delta v$
g	AU	degrees	AU	degrees	g s^{-1}/km s^{-1}
0.6	0.25	>45	0.1	1.5	$> 10^{13}$
0.7	0.3	35	0.1	1.3	6.5×10^{12}
0.8	0.4	17.5	0.2	1.0	6.5×10^{12}
0.9	0.6	10	0.05	0.6	9.3×10^{11}
0.95	1.0	4	0.125	0.4	9.3×10^{11}
0.98	1.75	2	0.04	0.2	1.5×10^{11}

So the mass of the comet tail is

$$M_{\rm ct} = \frac{r\rho\alpha l_0 L}{3Q_{\rm sca}} \tag{30}$$

We adopt $Q_{\rm sca} = 1$ for diffraction, a dust size of $r = 1\mu$m, and a density *inside the grains* of $\rho = 1$ g.cm^{-3}.

The dust production rate of the comet, P in g.s^{-1} is related to the mass of the comet tail

$$P = \frac{M_{\rm ct}}{t_{\rm ct}} = \frac{M_{\rm ct}\Delta v}{L} = \frac{r\rho\alpha l_0 \Delta v}{3Q_{\rm sca}} \tag{31}$$

where $t_{\rm ct}$ is the duration of the dust production rate, and Δv is the velocity of the dust relative to the head of the comet. Notice that the production rate is independent of the mass of the comet tail. We will see later that the mass is not constrained by the fit to the lightcurve, but the ratio $P/\Delta v$ is.

5.4. Lightcurves of the cometary cloud model

We have calculated the lightcurves due the passage of a triangular comet cloud and compared them with the observed light curve. The free parameters for any value of the scattering phase function, characterized by g, are the distance d, the angle α, the length L, the distance l_0 where the vertical optical depth reaches a value of $\tau(l_0) = 1$ and the impact parameter $b = t.d$ (in R_*) of the nucleus of the comet when it passes in front of the star. From these data we can also derive the mass of the comet-dust.

Similar to the spherical cloud, discussed above, the duration of the brightness increase is mainly determined by g and d. The amplitude of the brightness increase is determined by the distance and total projected surface of the dust $\Sigma_{\rm sca}$, i.e. by the combination of l_0, α and L. The duration of the dip in the lightcurve is determined by d and b. The depth of the dip is determined by b, α and l_0. The parameters of the best fitting models are listed in Table 3. For $g < 0.7$ we did not find a satisfactory fit to the observed lightcurve.

Fig. 7 shows a comparison between the observed and predicted lightcurve for the best fitting model. This best fitting model, with $g = 0.8$, has a projected scattering surface of $\Sigma_{\rm sca} = 7 \times 10^{25}$ cm^2 and a mass of 2×10^{21} g.

From this fitting of the observed with the predicted lightcurve we conclude that the cometary cloud model can explain the observed light curve of β Pic if it has the following characteristics.

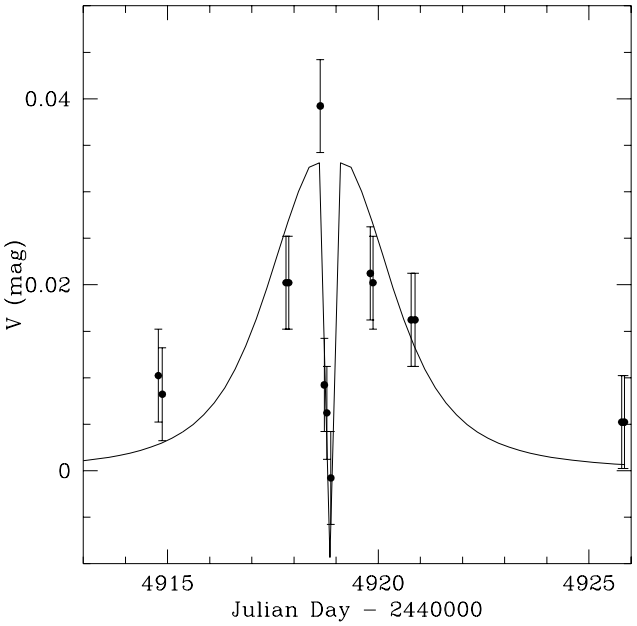

Fig. 7. The computed light curve for the best fit cometary cloud model with $g = 0.8$ compared with the observed lightcurve. The other parameters of this model are listed in Table 3

1. The short duration of the brightening requires the cloud to pass close to the star where the angular velocity is large. This is reflected in the values of d that was derived from the fit. The best fit requires a distance of about 0.4 AU.
2. The brightening requires a sufficient projected scattering surface of the comet cloud. Our best fitting model has $\Sigma_{\rm sca} = 7 \times 10^{25}$ cm^2. This is about a factor ten larger than the value derived from the spherical cloud model, because in the comet model the dust is distributed over a larger distance range.
3. The dip in the lightcurve requires that the cloud covers at least 6 percent of the stellar disk. The optically thick region must be large enough to produce an effective occultation. In our best fit model an optical depth of $\tau(l_0) = 1$ is reached at a distance of $l_0 = 0.2$ AU.
4. The short duration of the dip requires that only the head of the comet moves in front of the stellar disk and not the much larger optically thin part. This is naturally explained by our pointed comet model which has the highest optical depth closed to the star.
5. The light curve only gives a lower limit to the length of the dust tail, because particles at large distances hardly contribute to the scattering. The lower limit of L is about several AU. This implies a mass of a few times 10^{21} g for the comet tail if we assume a dust size of about 1 μm.
6. The optical depth rate is well constrained by the modeling. Assuming the same dust size, we find a dust production rates on the order of 10^{11} to 10^{13} g.s^{-1} for the canonical dust velocity of $\Delta v = 1$ km.s^{-1} (Spinrad, 1987). A higher dust velocity, e.g. due to radiation pressure, requires a higher dust production rate.

6. Summary and discussion

We have explained the fast variations in the optical light curve of β Pic near JD 4918 in terms of a scattering dust cloud that orbits the star. The forward peaked phase function for scattering or diffraction produces an increase in the brightness when the optically thin part of the cloud pass the line of sight to the star. The occultation of the stellar disk by the optically thick part of the cloud produces the dip in the light curve.

We adopted Henyey-Greenstein phase functions with g as a free parameter. For Zodiacal dust $g \simeq 0.64$. If the dust particles are diffracting, the value of g can be much larger. Calculations of the phase function for two mixtures of diffracting particles with radii of a few microns results in very strongly forward peaked phase functions with $g \simeq 0.90$ and 0.96 in the V-band. The forward scattering is even larger in the U-band.

We first derived some simple estimates for a spherically cloud with an optically thin nucleus and an optically thick outer envelope. This simple model can explain the brightness increase if the optically thin region has an effective scattering surface on the order of 10^{24} cm^2 (Table 2). Assuming a mean size of the dust particles of a few microns and a density of 1 g cm^{-3} the find that the optically thin part of the cloud has a mass of about 10^{21} g or 10^{-8} earth masses. Much more mass can be hidden in the optically thick part of the cloud.

The narrow absorption dip requires that the cloud is very optically thin $\tau < 10^{-2}$. The combination of the effective scattering surface and the small optical depth implies a geometrically large cloud with a radius on the order of 50 R_*. Such a large cloud will not be spherical but elongated and flattened. Therefore we also calculated light curves due to forward scattering in a cometary cloud.

In this case the optical thick part of the cloud (the comet head) is closest to the star. This can explain the short duration of the dip in the light curve because the extended optically thin region does not occult the star if the orbit is slightly tilted. The brightening of the star depends on the effective scattering surface and hence on the dust production rate for which we derive a range of $10^{11} < P/\Delta v < 10^{13}$ g.km^{-1} depending on the distance. The high dust production rate and the short duration of the dip suggest that the comet was close to the star near periastron.

The dust production rate is about seven orders of magnitude larger than observed from a single comet of the solar system (Spinrad, 1987). Even for large g corresponding to the diffracting part of the phase function, the calculated production rate is very large. Only a large number of fragments from a disrupted massive body can account for this amount of dust.

The observations show that the amplitude of the lightcurve in the U-band is larger than in the V-band (see Fig. 1). This might be due to diffracting dust particles. The phase functions for diffraction (Fig. 5) show that that $P(0)$ is about twice as high at 3500 Å than at 5000 Å. So the presence of diffracting particles can explain the higher peak in the U band than in the V band. The fact that this $U-B$ peak occurred near the center of the photometric event agrees with the relative shapes of the phase functions for diffraction in the U and B bands.

We conclude that the event in the lightcurve of β Pic near JD 4918 can be explained by scattering of a passing elongated dust cloud: an elongated proto-planet or a comet or series of comets like Shoemeker-Levi. If the cloud is due to a proto-planet, the event should be periodic. Photometric monitoring up to now has resulted in excluding a period of about 100 days, i.e. an orbiting cloud at a distance of about 0.5 AU (Section 1).

The discovery of the event in the very limited photometric data of β Pic that existed until 1982, suggests that it may be rather common. Therefore, photometric monitoring of β Pic to determine the frequency of such events is highly recommended. Such monitoring will result in much stronger constraints on the model and prove or exclude the proto-planetary cloud.

Acknowledgements. We thank Joop Hovenier for discussion on the scattering and diffraction properties of the dust, and the referee Chris Burrows for useful comments and suggestions.

Appendix A

The effective scattering surface of a sphere of radius $r_{\rm max}$ is defined by

$$\Sigma_{\rm sca} = \int_0^{r_{\rm max}} \left\{1 - e^{-\tau_{\rm sca}(p)}\right\} 2\pi p dp \tag{A1}$$

where $\tau(p)$ is the optical depth for a light of sight of impact parameter p through the sphere. For dust particles with a mean radius a the optical depth for scattering is

$$\tau_{\rm sca}(p) = N(p) \cdot \pi a^2 Q_{\rm sca} \tag{A2}$$

where $N(p)$ is the number of particles in the column at p through the cloud and $Q_{\rm sca}$ is the scattering efficiency. The effective scattering surface of the optically thick and thin regions of the cloud are defined by

$$\Sigma_{\rm sca}^{thick} = \int_0^{p_1} \left\{1 - e^{-\tau_{\rm sca}(p)}\right\} 2\pi p dp \tag{A3}$$

and

$$\Sigma_{\rm sca}^{thin} = \int_{p_1}^{r_{\rm max}} \left\{1 - e^{-\tau_{\rm sca}(p)}\right\} 2\pi p dp \tag{A4}$$

where p_1 is the impact parameter where $\tau_{\rm sca}(p) = 1$.

The optical depth for extinction is

$$\tau_{\rm ext}(p) = N(p) \cdot \pi a^2 Q_{\rm ext} = N(p) \cdot \pi a^2 Q_{\rm sca}/A \tag{A5}$$

where A is the albedo. The effective extinction surfaces $\Sigma_{\rm ext}$, $\Sigma_{\rm ext}^{\rm thick}$ and $\Sigma_{\rm ext}^{\rm thin}$ are defined analogously to Eqs. A1, A3 and A4.

The effective surface for occultation when the cloud is (partly) in front of the star is

$$\Sigma_{\rm occ} = \int_{\rm occ} \left\{1 - e^{-\tau_{\rm ext}(p)}\right\} ds \tag{A6}$$

where ds is a surface element of the cloud as seen by the observer and the integration is over the occulting area of the cloud. This

integral can be split into an optically thick and and optically thin part, where $\tau_{\rm ext}(p) > 1$ or < 1 respectively.

$$\int_{\rm occ(\tau>1)} \left\{1 - e^{-\tau_{\rm ext}(p)}\right\} ds \simeq \int_{\rm occ(\tau>1)} ds = \Sigma_{\rm occ}^{\rm thick} \qquad \text{(A7)}$$

and

$$\begin{aligned} \int_{\rm occ(\tau<1)} \left\{1 - e^{-\tau_{\rm ext}(p)}\right\} ds &= \left\{1 - e^{-<\tau_{\rm ext}>}\right\} \int_{\rm occ(\tau<1)} ds \\ &\equiv \left\{1 - e^{-<\tau_{\rm ext}>}\right\} \Sigma_{\rm occ}^{\rm thin} \qquad \text{(A8)} \end{aligned}$$

where $< \tau_{\rm ext} >$ is the mean extinction optical depth of the occulting optically thin area. For other geometries the definitions are analogous.

References

Artymowicz P.,1995, *in* Circumstellar Dust Disk and Planet Formation, R. Ferlet & A. Vidal-Madjar Eds, Editions Frontières
Aumann H.H., Gillett F.C., Beichman C.A., et al., 1984, ApJ 278, L23
Crifo, F., Vidal-Madjar, A., Lallement, R., Ferlet, R., Gerbaldi, M., 1997, A&A 320, L29
Golimowski D.A., Durrance S.T., Clampin M., 1993, ApJ 411, L41
Hong S.S., 1985, 1985, A&A 146, 67
Kalas P., Jewitt D., 1995, AJ 110, 794
Lagage P.O. & Pantin E., 1994, Nature 369, 628
Lanz T., Heap S.R., Hubeny I., 1995, ApJ 447, L41
Lecavelier des Etangs A., 1996, PhD Thesis, Paris University.
Lecavelier des Etangs A., Deleuil M., A. Vidal-Madjar A., et al., 1995, A&A 299, 557
Lecavelier des Etangs A., Vidal-Madjar, A., Burki, G. et al., 1996, Paper I, A&A, (in press)
Paresce F., Burrows C., 1987, ApJ 319, L23
Pollack J.B., Cuzzi J.N., 1980, Journ. Atmos. Sc. 37, 868
Smith B.A., Terrile R.J., 1984, Sci 226, 1421
Spinrad, H. 1987, ARA&A 25, 231

This article was processed by the author using Springer-Verlag LaTeX A&A style file *L-AA* version 3.